Research Article

Journal of Environmental Nanotechnology

Empirical and ANN Optimization Study on Lemongrass Oil Blends in CI Engines

S. Vinodraj*, N. Sethuraman, R. Prabhakaran, R. Thamizhvel, A. Shabeer and S. Jagathesh

Department of Mechanical Engineering, IFET College of Engineering, Villupuram, TN, India

Received: 15.03.2025 Accepted: 05.06.2025 Published: 30.06.2025

*vinodhraj.raj3@gmail.com

ABSTRACT

This research investigates the efficiency and exhaust characteristics of a CI engine operating with a B20 lemongrass oil biodiesel mixture, systematically exploring the intricate interactions between compression ratios (17.5 and 18.5), injection pressures (220-260 bar), and injection timings (22°-26°bTDC. Leveraging an ANN optimization framework, the study aims to comprehensively analyze and define the experimental parameters. Experimental findings reveal that diesel (F0) outperforms lemongrass oil biodiesel (F1) in BTE and Brake specific fuel consumption (BSFC), with Brake Thermal Efficiency ranging from 27.46%–29.5% and BSFC of 0.29–0.32 kg/kWh, compared to biodiesel's 25.7%–28.4% and higher BSFC of 0.34–0.44 kg/kWh. Diesel also produces lower CO (0.4166%–0.4877%) and NOx (230.45–249.23 ppm), while biodiesel emits higher CO (0.45%–0.59%) and NOx (233.56–249.56 ppm). Biodiesel (F1) has lower HC emissions (47.8–51.9 ppm) but higher smoke opacity (53.9%–58.96%) compared to diesel's higher HC (51.9–63.5 ppm) and lower opacity (54.2%–56.23%). Using an ANN model with Bayesian optimization and activation functions (tanh, sigmoid, ReLU), the study found that predicted values closely align with actual values, with minimal deviations for BTE and HC emissions. However, larger deviations are observed for BSFC and NOx, especially at higher values. Improvements are recommended to enhance prediction accuracy for BSFC and NOx.

Keywords: Lemon grass oil; Performance emission; Optimization; ANN.

1. INTRODUCTION

Diesel engines are a key power source, extensively used in industries like defence, automotive, mining, and maritime, owing to their superior fuel efficiency and robust performance. However, given the existing fossil fuel reserves and the rising rate of consumption, these resources are steadily approaching depletion. Consequently, the exploration and development of sustainable energy sources have become critical. Biofuels are garnering global appeal as an effective supplement for conventional fuels (Arunprasad *et al*. 2018; Dwivedi *et al*. 2014; Datta *et al*. 2014). Although biofuels exhibit lower efficiency compared to petroleum-based fuels, they are intensely preferred due to their diminished emissions. Furthermore, biofuels can be blended with diesel in specific ratios for use in engines, without the need for major tweaks to the engine's structure. Biofuels share similar combustion and thermal properties with diesel, but they have a much greater oxygen concentration. Biofuels are categorized into 3eras based on their feedstock: 3rd eras biofuels come from microalgae and macroalgae, 2nd- eras biofuels come from non-food feedstocks, and first-generation biofuels from edible feedstocks. While experimental studies are crucial for fully understanding engine performance with biofuels, there is a growing tendency to use various simulation methods to replicate engine behaviors. To reduce costs, exploration time, and trials, linear and nonlinear algorithms, including ANN, factorial design, genetic algorithms, and RSM, are used to analyze engine behaviors (Krishnamoorthi *et al*. 2018). When compared to the RSM model, ANN offers more steadfast predictions and displays an elevated correlation between observed and predicted results, making it a powerful learning approach (Babu *et al*. 2020). The implementation of advanced ANN-based modeling represents a major step forward in the numerical evaluation of CI engine characteristics. The implementation of advanced ANN-based modelling represents a major step forward in the numerical evaluation of CI engine characteristics. The performance of Ricinus communis seed biodiesel was predicted using an Artificial Neural Network (ANN) framework. Orange peel oil-diesel blends were also investigated as a potential alternative to conventional diesel in compression ignition (CI) engines. For a blend consisting of 70% diesel and 30% orange peel oil, Brake Specific Energy Consumption (BSEC) decreased by 19%, while Brake Thermal Efficiency (BTE) increased by 16.5% at peak load. An ANN model was created using the Quasi-Newton algorithm, with R^2 values of 0.986 for BSEC and 0.994 for BTE. (Bahri *et al*. 2017) demonstrated that the Neural Network model can be effectively used as a practical tool for engine actions, accurately predicting burning noise levels with less than 0.5 percent deviation.

(Channapattana *et al.* 2017) examined the performance of honing oil-derived biodiesel in CIDI engines at different concentrations (20% to 100%). They utilized ANN simulations to assess experimental results, focusing on outputs such as thermal efficiency, exhaust gas temperature, carbon monoxide, hydrocarbons, nitrogen oxide, fuel consumption, and smoke. To optimize the training process, they used algorithms like train(scg), train (gdx), train(rp), and train(lm). Their findings indicated that the hidden layer holds 28 neurons provided the best correlation and least MSE when using the train (lm) algorithm.

This study presents a novel investigation into the utilization of Lemongrass oil biodiesel as an alternative fuel, addressing a significant gap in existing literature concerning its performance and emission characteristics in compression ignition engines. In addition, the work advances the current state of research by implementing an Artificial Neural Network (ANN)-based predictive model for engine performance analysis, offering a data-driven approach that has seen limited application in this context. The research is divided into 2stages. The first phase examines the impact of Lemongrass oil biodiesel blends, SB20 and SB0, on exhaust (NOx, smoke, and HC) and efficiency (BTE and SFC) in a CI engine. The 2nd phase focuses on developing a Neural Network model to precisely predict CI engine response. The Neural Network model was created using MATLAB software, and the study examines how factors like training algorithms, epochs, transfer function types, and the number of neurons impact the model's prediction reliability.

2. MATERIALS AND APPROACHES

2.1 Test Rig and Fuel Properties

This research investigated the use of diesel and biodiesel resulting from Lemongrass oil as potential replacements for fuel in compression ignition (CI) engines. Pure diesel (F0: 100% diesel) was used as a reference to compare fuel attributes such as viscosity, flash point, calorific value, and density. The tested fuels included F1 (a blend of 80% Lemongrass biodiesel and 20% diesel) and F0 (100% diesel), measured by volume. The physicochemical properties of these fuels, outlined in Table 1, were evaluated, rendering them to ASTM standards. The chemical composition of lemongrass oil biodiesel primarily consists of fatty acid methyl esters (FAME) derived from the transesterification of the oil's triglycerides. Typical major components include Methyl linoleate (C18:2) Methyl palmitate (C16:0) Methyl oleate (C18:1) Methyl stearate (C18:0).

2.1.1 Biodiesel Preparation and Production

Crude lemongrass oil was extracted using a mechanical screw press expeller, resulting in the presence of minor impurities such as suspended organic matter, trace water content, and other residual contaminants. Prior to transesterification, the oil was filtered to remove particulates and preheated to facilitate moisture evaporation, ensuring improved reaction efficiency. The transesterification process as shown in figure1 was performed using a base-catalyzed single-step reaction, wherein the triglycerides present in the lemongrass oil were chemically converted into fatty acid methyl esters (FAME) in the presence of methanol and a catalyst. Sodium methoxide (CH_3ONa) was utilized as the homogeneous catalyst at a concentration of 3.5 g per liter of oil, while methanol (CH_3OH) was added at a ratio of 250 mL per liter of oil, corresponding to an approximate 6:1 molar ratio of alcohol to oil.



Fig. 1: Transesterification of Lemon grass oil

The reaction was carried out in a jacketed stainless-steel batch reactor with a capacity of 40 liters. The oil was initially heated and maintained at a controlled temperature of 65–70 °C, which lies near the boiling point of methanol, to enhance the reaction kinetics while avoiding methanol vaporization. The mixture was stirred continuously at 600 rpm for a duration of 90 minutes to ensure thorough mixing and optimal mass transfer. Upon completion, the mixture was allowed to settle under gravity to separate the ester (biodiesel) and glycerol phases.

Table 1.Physiochemical properties of Lemon grass biodiesel and diesel

Fuel Properties	Diesel (F0)	Lemon Grass Biodiesel (F1)
Kinematic viscosity, cSt at 40°C	4.1	56.4
Specific gravity at 15°C	0.85	0.96
Flash point°C	58	94
Fir point °C	67	101
Calorific value kJ/kg	44512	41422
Density, kg/m3	832	910
Cetane number	42	50

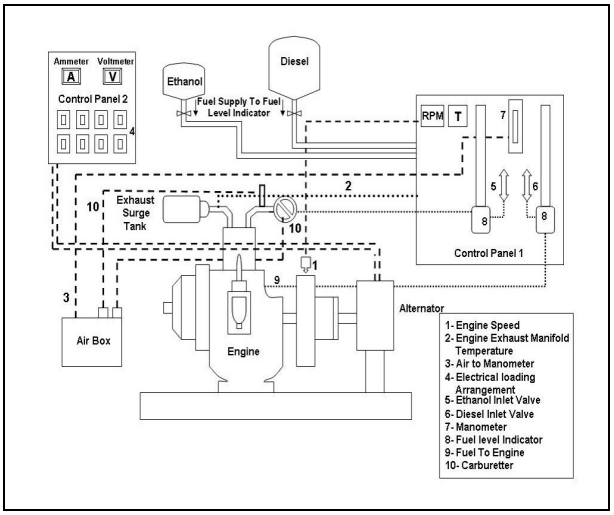


Fig. 2: Graphic form of test rig

The analysis was carried out on a compression ignition, 4-stroke, mono-cylinder, and water-cooled engine to examine the outcomes of lemongrass biodiesel blends on exhaust and efficiency limits. The mechanical details of the test engine utilized in the study are detailed in Table 2, while Figure one demonstrates the layout diagram of the engine arrangements. During the experiments, the injection timing was varied between 22° and 26° bTDC, and the injection pressure ranged from 220 to 260 bar. The engine load was adjusted from 0 to 10 kg, with the rotational speed maintained consistently at 1500 rpm. The test setup covered components such as a multi-gas analyzer, a fuel control valve, separate fuel tanks for diesel and lemon grass biodiesel, an air filter, an eddy current dynamometer, a rotameter, and an air box.

During experimentation:

- The different types of levels and parameters taken into account for the experimentation and optimization are given in Table 3
- The lubrication, cooling system, and fuel system were thoroughly checked to ensure correct functionality.
- To establish stable, functional conditions, the engine was operated deprived of load for 30 minutes using diesel as the baseline fuel.
- Relevant data were meticulously recorded through physical measurements. The parameter ranges (17.5–18.5 CR, 220–260 bar IP, and 22°–26° bTDC IT) were selected based on prior literature, engine manufacturer guidelines, and preliminary experimental trials. These ranges ensure safe engine operation while capturing the influence of key combustion variables. They are commonly employed for biodiesel-fueled CI engines to optimize performance and emissions using F1 (lemongrass oil) and F0 (diesel) fuels. Emission levels and performance parameters were carefully measured and analyzed.
- HC and NOx gases were measured in parts per million, while CO levels were recorded in percentages.

Table 2. Engine specifications and emission analyzer measurement range

Model	Kirloskar, TV1
Type of Engine	Four-stroke, direct engine, water-cooled, VCR engine.
Bore × Stroke	87.5 mm × 110 mm
Power	5.2 kW @ 1500 rpm
Displacement	661 cm3
CR	17.5:1 standard & 15:1 – 18:5 (VCR)
Loading Mechanism	Eddy current dynamometer
Load Measurement sensor	Strain gauge type load cell, range 0–50 kg
Sensor - pressure	resolution 0.1 psi, range 0–5000 psi, Strain gauge type,
Software	Performance analysis software for engine and dynamometer specifications

3. ARTIFICIAL NEURAL NETWORK

An artificial neural network is an analytical model that replicates the functions of the human neuro-system (Chizoo *et al*. 2019). These networks are versatile tools capable of performing tasks such as memorization, inference, decision-making, and learning. Neurons serve as the core components of an ANN. While training, the structure of the network can adapt and update, rooted in the flow of output-input data through it (Ramalingam *et al.* 2020). Because of its nonlinear properties, ANN is particularly effective for solving problems involving complex mathematical relationships (Ilangkumaran *et al.* 2016). Data gathered from steady test trials was used to construct model ANN. The proposed ANN methodology is presented in Figure 2 for predicting the exhaust and efficiency of a Compression Ignition engine using (F0 and F1 fuels). Since the effectiveness of an ANN depends heavily on the quality of its input data, it is vital to scale both input and output variables. The Min-Max Scaler preprocessing technique (Equation (1) (Soukht *et al.* 2017) was employed to normalize these variables. This normalization process ensures equal importance is assigned to all output and input data, preventing metrices

with elevated data from dominating those with lower values during ANN training.

$$X_{pre-processing} = \frac{X - X_{min}}{X_{max} - X_{min}} \quad \ldots (1)$$

Here, Xmin and Xmax represent the maximum and minimum data of the indicators, while X is the parameter data to be normalized. The dataset was normalized within the range of 0 to 1. The data was arbitrarily divided into proportions of 15%, 70%, and 15 percent for testing, validation, and training of the model subsequently.

Using MATLAB, the ANN model was constructed, and its performance was evaluated across different conditions by altering the activation functions, number of neurons in the hidden layer, optimizer, and epochs. The outcome variables included NOx, HC, CO2, SFC (kg/kWh) and BTE (%). Input variables consisted of IT, IP, CR, and fuels tested used. An optimizer is an algorithm designed to adjust ANN parameters, such as learning rate and weights, to minimize loss. The optimizers evaluated are Adam (a stochastic gradient descent method that uses adaptive estimates of first and second-order moments), Nadam (which incorporates Nesterov momentum) and Adam (a stochastic gradient descent method that uses adaptive estimates of first and second-order moments)

The activation or transfer functions analyzed include ReLU (which returns either zero or the maximum value), Sigmoid (which yields outputs between 0 and 1), and Softmax (which produces output vectors within the range of 0 to 1). The activation function is essential in shaping the output of the ANN model.

The number of neurons in the network's hidden layer varied from 8 to 32, increasing in steps of 8 (i.e., 8, 16, 24, and 32). A single hidden layer was used for the ANN analysis, with the number of epochs set between 200 and 800, in increments of 200 epochs (i.e., 200, 400, 600, and 800). The trained neural network was simulated for all input data to create consistent outcomes. The efficiency of the network was evaluated using the r and MSE. The correlation coefficient (r) is used to assess the strength and direction of relationships between variables, with positive (upward) and negative (downward) signs indicating the direction. Correlation indicators ranging from 0.3 to 0.7, 0.7 to 1.0 and 0 to 0.3 are classified as weak, moderate, and strong respectively (Vinod and Dheikshith, 2023) The net with the smallest error validation loss is considered the most preferable.

The prime fit of the line is represented by data closer to zero. The inquiry of the ANN network involves the following steps:

- Specifying output and input parameters.
- Preprocessing outcome and input data.
- Configuring the optimizer, activation function, number of epochs and hidden layers.

Step 1: The tanh activation function with Bayesian optimizer was selected and assessed for different numbers of neurons in the epochs and hidden layer. The Bayesian optimizer and Tanh activation function were fixed; four iterations were performed for each configuration of neurons in the hidden layer.

Step 2: The results, including MSE and r training, along with Validation of MSE and r for the output variables, were organized into tables and plotted.

These steps were repeated using the Bayesian optimizer with other activation functions, specifically tanh, sigmoid and ReLU.

Table 3. Different levels and parameters used in the experimentation

Symbols	Design Factor	Units	No of Levels	Levels		
X1	IP bar	Bar	3	220	240	260
X2	IT	bTDC	3	22	24	26
X3	CR	No unit	2	17.5	18.5	-
X4	Fuel used	No unit	2	F0 (Diesel)	F1 (lemon grass biodiesel)	-

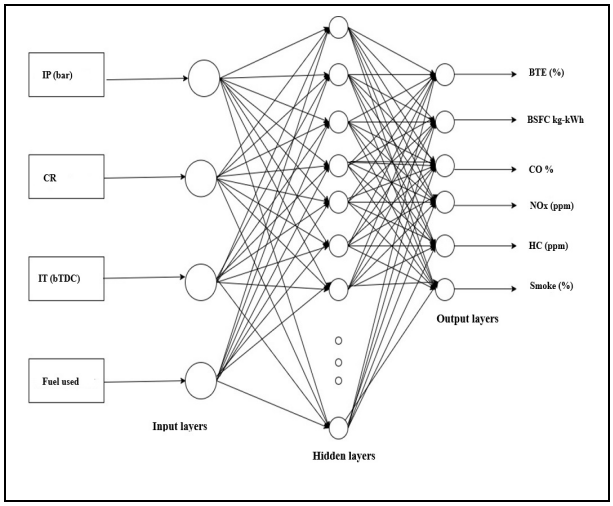


Fig. 3: Proposed ANN configuration

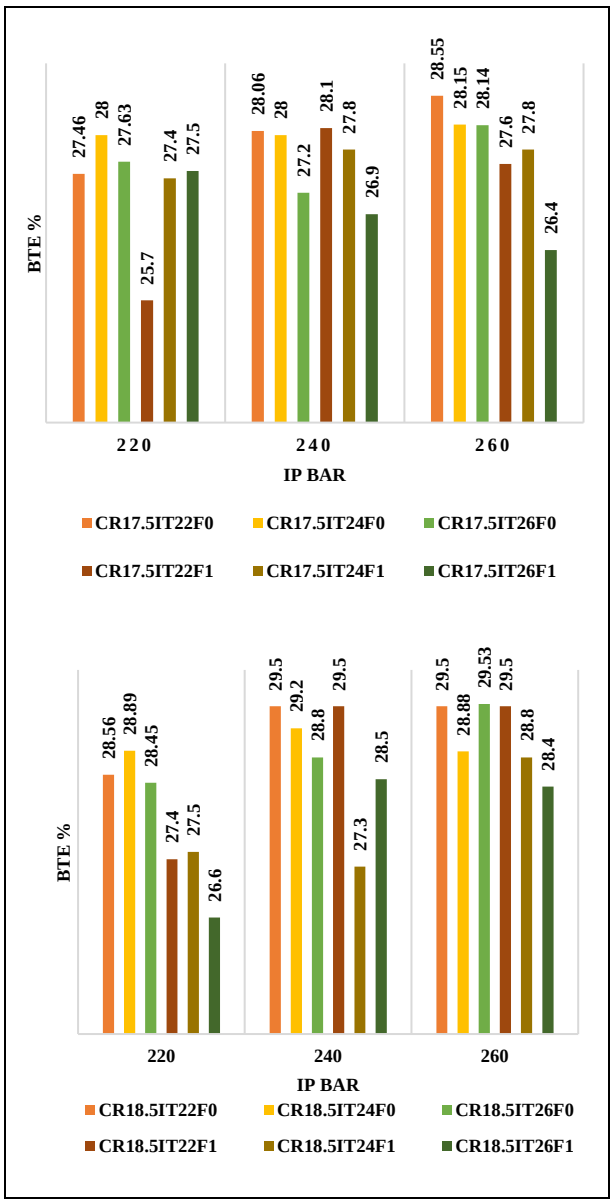


Fig. 4: Illustrates: history of BTE against IP (bar)

4. EXPERIMENTAL RESULTS

4.1 Impact of BTE for CR 17.5 & 18.5

The relationship between injection pressure (IP) and brake thermal efficiency (BTE) (figure 4) in a CI engine fuelled with lemongrass biodiesel shows diesel consistently achieving higher BTE than lemon grass biodiesel. At 220 bars, with a CR of 18.5 or 17.5 and injection timing (IT) of 22°–26° bTDC, diesel achieves a BTE of 27.46%–28.63%, attributed to its higher heating value and better atomization, while lemon grass biodiesel reaches 25.7%–27.5% due to higher viscosity and lower volatility. At 240 bars, diesel achieves 28.06%–29.5%, while lemon grass biodiesel peaks at 29.5% but drops to 26.9% due to over-atomization and heat losses. At 260 bars, diesel maintains superior efficiency at 28.55%–29.5%, while lemon grass biodiesel declines to 26.4%–28.4%. Optimal IT and CR enhance BTE by improving combustion timing with air-fuel mixing, benefiting diesel more. Higher IP promotes complete combustion, reducing CO and HC emissions but increasing NOx. While lemongrass biodiesel performs competitively, diesel's combustion properties provide consistently higher BTE across varying Ips (Maurya *et al.* 2018)

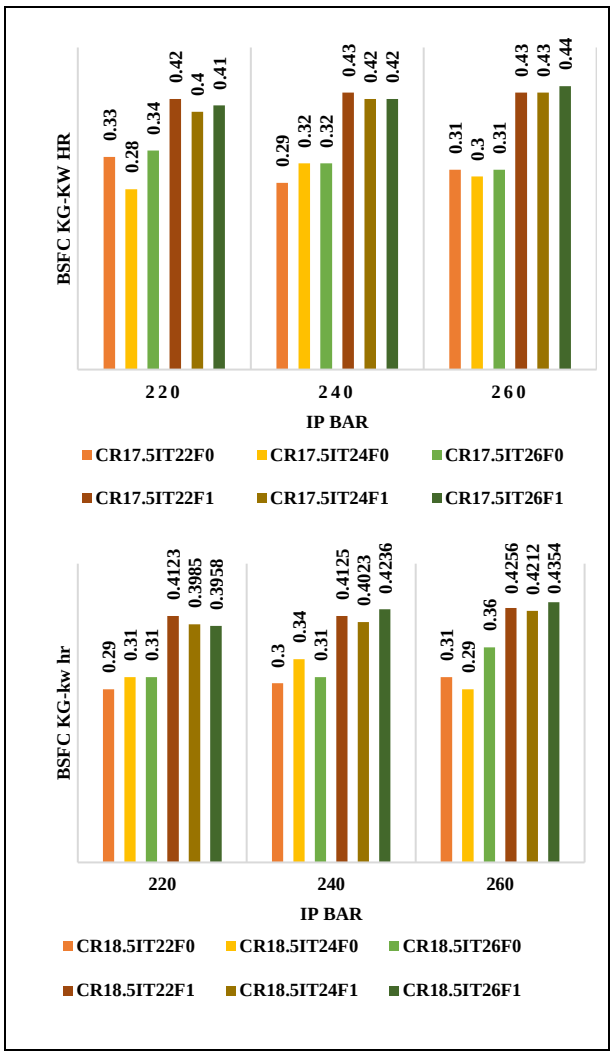


Fig. 5: Illustrates: history of BSFC (kg-kW hr) against IP (bar)

4.2 Impact of BSFC (kg-kW hr) for CR 17.5 & 18.5

The graph (figure 5) shows BSFC for F0 (diesel) and F1 (lemon grass biodiesel) at different injection pressures. At 220 bars, diesel achieves BSFC values of 0.33–0.41 kg/kWh, while lemon grass biodiesel ranges from 0.34–0.42 kg/kWh, with higher BSFC for lemon grass biodiesel because of its lessened energy content and elevated viscosity. At 240 bars, F0 improves to 0.29–0.32 kg/kWh, while F1 slightly decreases to 0.42 kg/kWh but still consumes more fuel. At 260 bars, F0 maintains efficiency at 0.30–0.31 kg/kWh, while F1 increases to 0.43–0.44 kg/kWh, reflecting challenges in efficient

combustion. Diesel consistently demonstrates lower BSFC across all pressures due to its higher energy density, better atomization, and combustion efficiency. Lemon grass Biodiesel's higher viscosity, oxygen content, and lower energy content lead to 14–35% elevated consumption of fuel for the same power output (Nirmala *et al*. 2020). While higher injection pressure improves atomization for both fuels, biodiesel's inherent limitations restrict efficiency gains. Thus, diesel remains more fuel-efficient under all conditions.

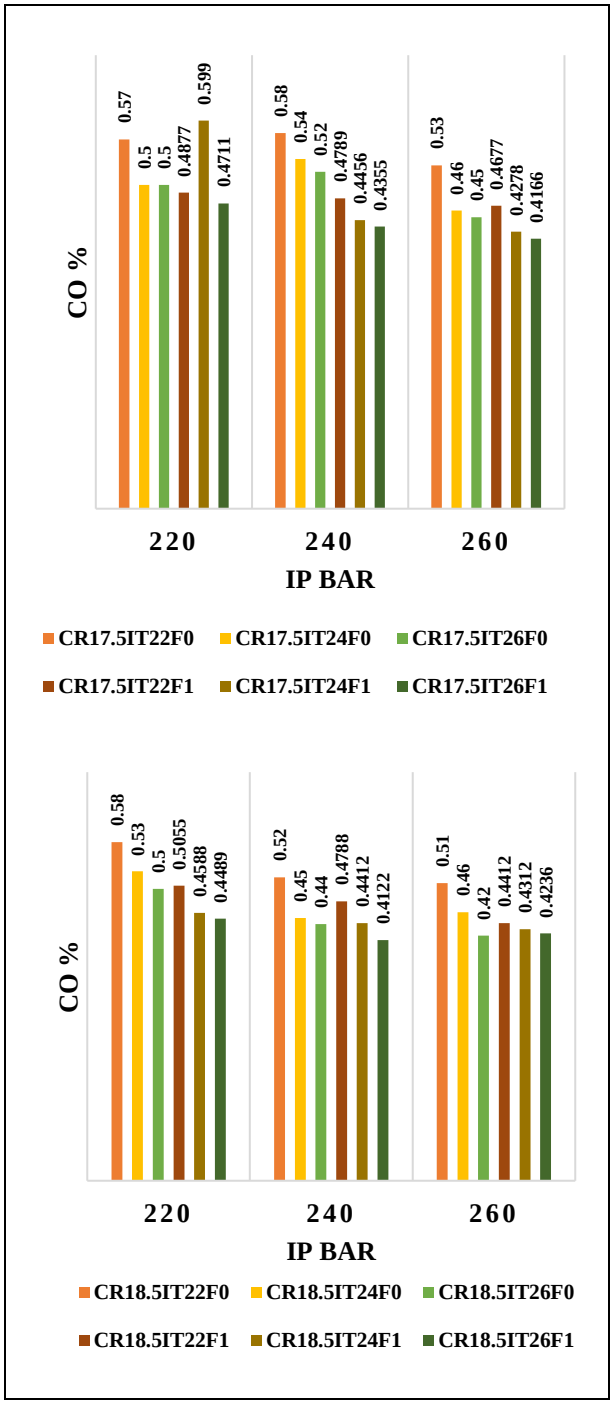


Fig. 6: Illustrates: history of CO % against IP (bar)

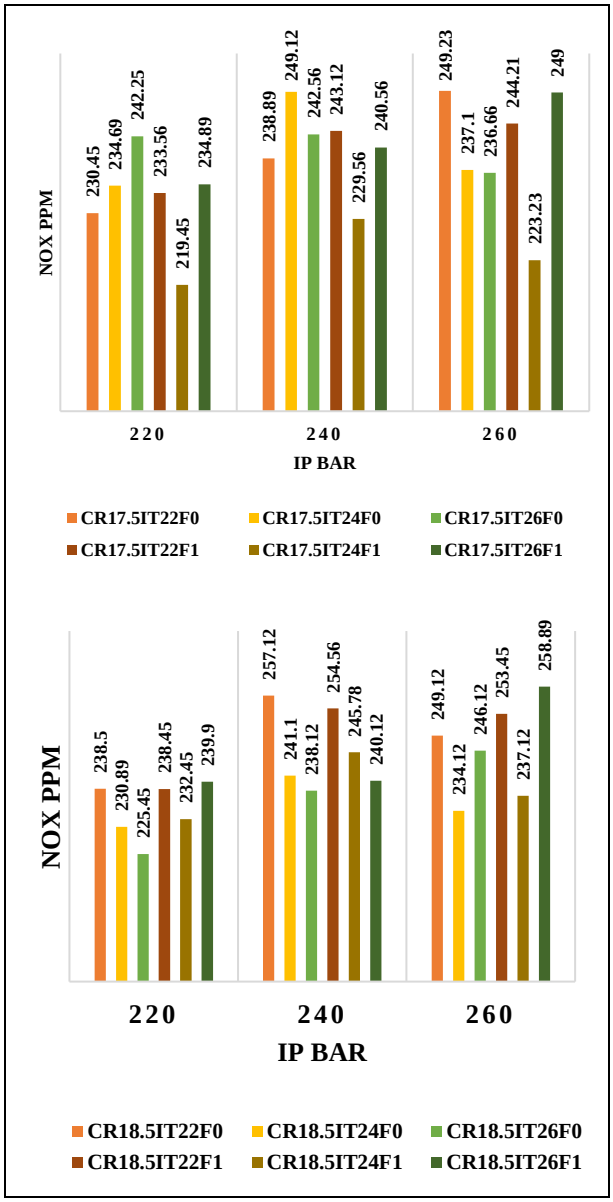


Fig. 7: Illustrates: history of NOx (ppm) against IP (bar)

4.3 Impact of CO for CR 17.5 & 18.5

The graph (Figure 6) compares CO emissions (%) for diesel (F0) and lemon grass biodiesel (F1) at injection pressures (IP) of 220, 240, and 260 bar, under compression ratios (CR) of 17.5 and 18.5. CO emissions decrease with increasing IP because of elevated atomization and superior fuel-air mixing, enhancing combustion efficiency. Diesel consistently emits less CO than biodiesel due to its lower viscosity, higher energy density, and superior combustion properties. At 220 bars, diesel emits 0.4585–0.4877%, while lemon grass biodiesel emits 0.53–0.59%, as lemon grass biodiesel's higher viscosity hinders atomization, causing incomplete combustion. At 240 bars, diesel improves to 0.4412–0.4589%, while lemon grass biodiesel reduces to 0.52–0.45%, benefiting from oxygen content but limited by

lower calorific value. At 260 bars, diesel achieves the lowest emissions (0.4166–0.4236%), while lemon grass biodiesel improves to 0.45–0.51%, though its oxygen-rich structure still limits complete combustion. The higher CR of 18.5 further reduces CO emissions for both fuels by increasing pressure and temperature, promoting more complete combustion (Yahya *et al*. 2020). Diesel's efficient atomization and combustion characteristics result in consistently lower CO emissions, while biodiesel's fuel properties restrict its ability to achieve similar reductions.

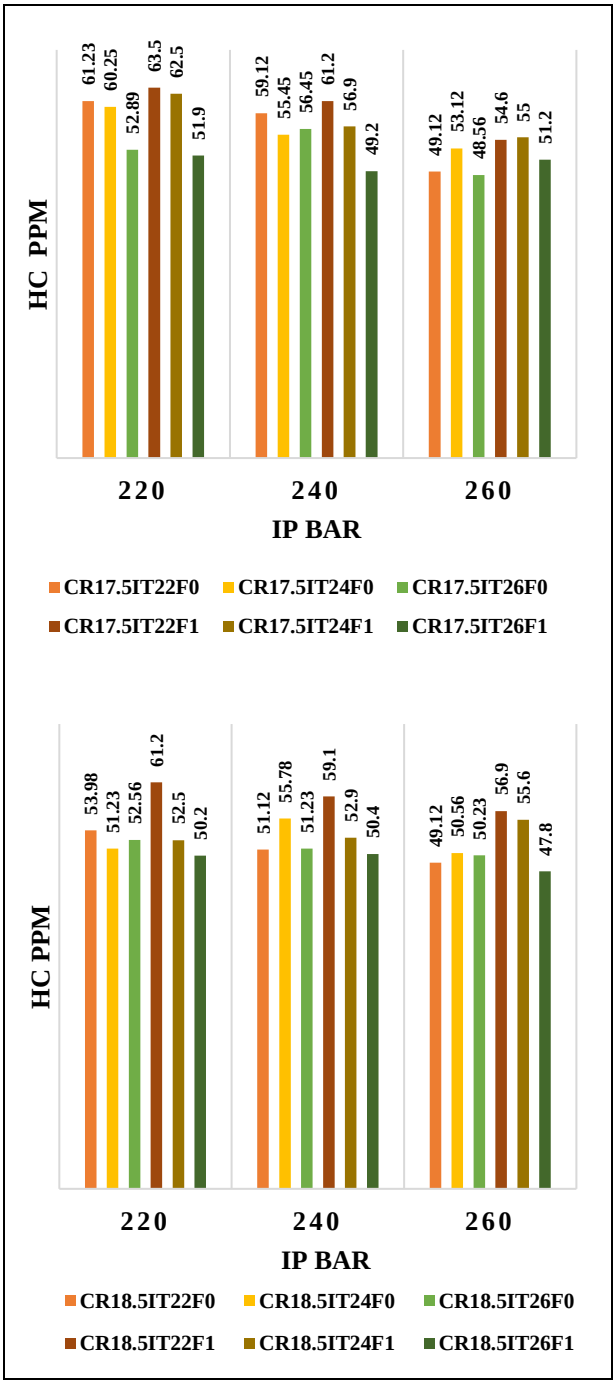


Fig. 8: Illustrates: history of HC (ppm) against IP (bar)

4.4 Impact of NO_x ppm for CR 17.5 & 18.5

The graph (Figure: 7) compares NOx emissions (PPM) for diesel (F0) and lemon grass biodiesel (F1) at IP of 260, 240&220 bar under compression ratios (CR) of 17.5 and 18.5. NOx emissions increase with higher IP because of better atomization and elevated burning temperatures. At 220 bars, diesel emits 230.45–234.69 PPM, while lemon grass biodiesel emits 233.56–242.25 PPM, with biodiesel's oxygen-rich composition leading to higher NOx. At 240 bars, diesel emissions rise to 238.89–245.12 PPM, while lemon grass biodiesel reaches 239.56–249.56 PPM. At 260 bars, diesel emits 237.71–249.23 PPM, while lemon grass biodiesel remains higher at 244.21–249.00 PPM. Advanced injection timing (IT26) further increases NOx due to higher peak combustion temperatures. Configurations like CR18.5IT22F0 exhibit the lowest emissions, whereas CR18.5IT26F1 shows the highest, reflecting the influence of injection timing and fuel blend. While lemongrass biodiesel produces more NOx due to its oxygen content, diesel's lower oxygen content limits peak temperatures, reducing emissions. Optimizing parameters such as IT, IP, and fuel blends could mitigate NOx emissions, balancing performance, and environmental impact (Teoh *et al*. 2021*;* Vinodraj *et al.* 2023*;* Shafay *et al*. 2022).

4.5 Impact of HC (ppm) for CR 17.5 & 18.5

The graph (Figure: 8) illustrates HC emissions (PPM) for diesel (F0) and lemon grass biodiesel (F1) across injection pressures (IP) of 220, 240, and 260 bar, highlighting the impact of combustion parameters. HC emissions decrease as IP increases, because of enhanced fuel atomization and air-fuel mixing at higher pressures. At 220 bars, CR17.5IT26F1 records the lowest emissions (51.9 PPM), while CR17.5IT26F0 has the highest (63.5 PPM). At 240 bars, CR17.5IT22F1 achieves the lowest emissions (49.2 PPM), and at 260 bars, CR17.5IT26F1 demonstrates the minimum (47.8 PPM), indicating optimized combustion with higher IPs and F1 blends. Advanced injection timing (IT26) increases HC emissions at lower IPs due to wall impingement and incomplete combustion. Lemon grass biodiesel (F1) generally shows reduced HC emissions due to its oxygen-rich composition promoting complete combustion. Increasing IP enhances spray characteristics, reducing unburned hydrocarbons (Dhar and Agarwal*,* 2018; Qi *et al.* 2010) Configurations like CR18.5IT26F1 consistently minimize HC emissions, showcasing their effectiveness. Optimizing IP, IT, and fuel blends is critical for clean and efficient engine performance.

4.5 Impact of Smoke (ppm) for CR 17.5 & 18.5

The graph (Fig. 9) shows smoke opacity percentages for diesel (F0) and lemon grass biodiesel (F1) across injection pressures (IP) of 220, 240, and 260

bar, influenced by injection timing (IT), nozzle geometry, and air-fuel mixing. At 220 bar, CR17.5IT26F1 has the highest opacity (58.96%), while CR17.5IT22F1 records the lowest (54.3%), reflecting better combustion efficiency. At 240 bar, opacity narrows, ranging from 54.2% (CR17.5IT22F1) to 56.23% (CR17.5IT26F0), showing improved atomization. At 260 bar, CR17.5IT26F1 again shows the highest opacity (58.89%), while CR17.5IT22F1 remains the lowest (53.9%). Higher IP enhances atomization and reduces opacity in optimal configurations like CR17.5IT22F1, which benefits from precise injection timing and nozzle design, ensuring efficient combustion (Silitong *et al.* 2018; Odufuwa *et al.* 2014). In contrast, CR17.5IT26F1 shows consistently high opacity due to factors like rich mixtures or poor air-fuel mixing.

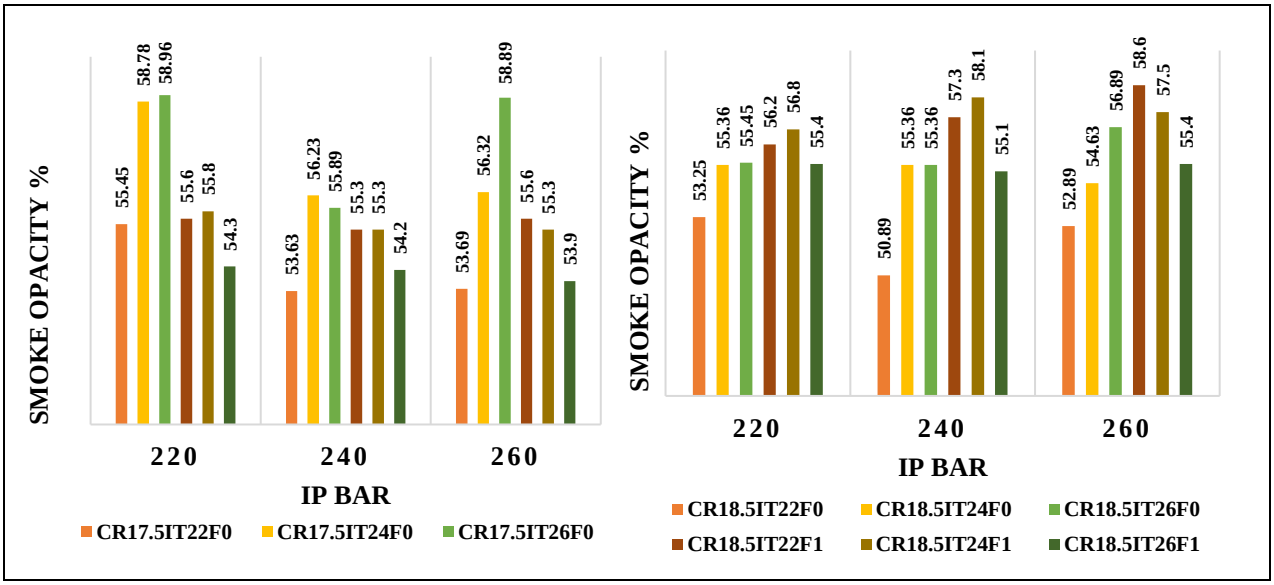
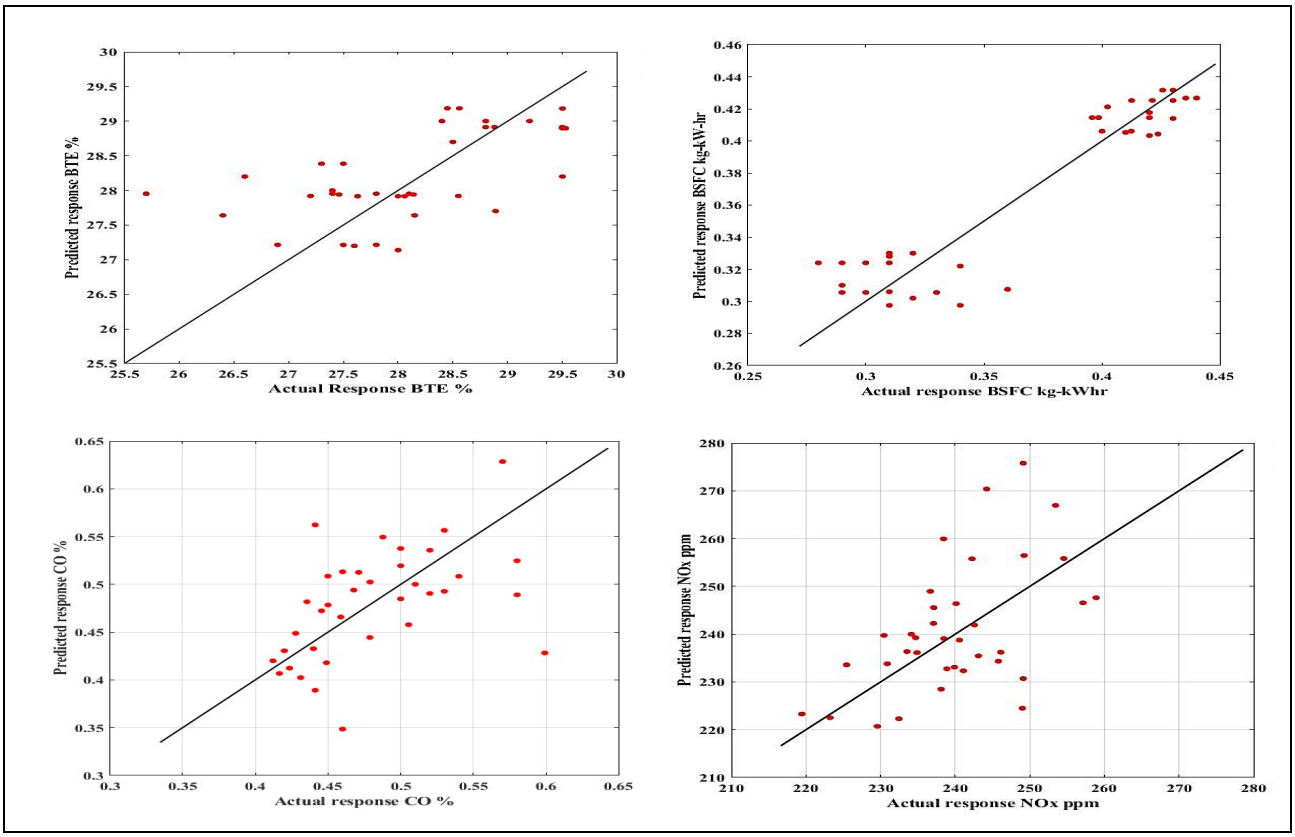


Fig. 9: Illustrates: history of smoke opacity (%) against IP (bar)

Table 4. MSE and r data of outcomes

					MSE train	MSE Val	MSE loss –Overall			
Optimizer	Activation Function	No. of Epochs	No. of Neurons in the Hidden Layer	Attributes	Loss	Loss	Tain	Val	Train r	Val r
Bayesian	tanh	200	8	BTE	0.001768	0.017794	0.002809	0.019736	0.8956	0.8456
				BSFC	0.008612	0.000875			0.8563	0.9125
				CO	0.001423	0.002784			0.8756	0.8756
				NOx	0.002041	0.008457			0.8456	0.9012
				HC	0.002451	0.008812			0.8900	0.8923
				Smoke	0.000564	0.000387			0.8345	0.8845
Bayesian	tanh	400	16	BTE	0.005452	0.022750	0.000449	0.005312	0.9612	0.9421
				BSFC	0.000410	0.000701			0.8860	0.9125
				CO	0.000588	0.000781			0.9255	0.9148
				NOx	0.001107	0.006242			0.8958	0.9785
				HC	0.000312	0.000412			0.9001	0.8945
				Smoke	0.000280	0.000541			0.8748	0.8889
Bayesian	tanh	600	24	BTE	0.002061	0.010612	0.000693	0.002605	0.99814	0.82234
				BSFC	0.000120	0.000351			0.99742	0.99345
				CO	0.000287	0.000548			0.99586	0.99457
				NOx	0.000542	0.002875			0.97451	0.96745
				HC	0.000541	0.001120			0.95842	0.94125
				Smoke	0.000612	0.000124			0.91258	0.89241
Bayesian	tanh	800	32	BTE	0.001394	0.022741	0.003699	0.005951	0.99701	0.82457
				BSFC	0.000125	0.000491			0.97458	0.994512
				CO	0.002578	0.001178			0.89471	0.98741
				NOx	0.000589	0.010276			0.91547	0.9147
				HC	0.004531	0.000482			0.90120	0.89562
				Smoke	0.000471	0.000540			0.94120	0.92145
Bayesian	sigmoid	200	8	BTE	0.005784	0.009781	0.001679	0.001860	0.97451	0.9012
				BSFC	0.000401	0.000356			0.95842	0.8923
				CO	0.001190	0.000378			0.91258	0.8845
				NOx	0.002140	0.000281			0.89582	0.82457
				HC	0.000260	0.000141			0.90012	0.994512
				Smoke	0.000300	0.000226			0.87485	0.98741

Bayesian	sigmoid	400	16	BTE	0.004521	0.0017450	0.008515	0.02656	0.99077	0.87451
				BSFC	0.004871	0.0117841			0.99875	0.99043
				CO	0.014520	0.0287412			0.89451	0.99647
				NOx	0.019710	0.0524101			0.91470	0.97561
				HC	0.007061	0.0164570			0.99412	0.82784
				Smoke	0.000410	0.0470001			0.98451	0.9818
Bayesian	sigmoid	600	24	BTE	0.006312	0.0094571	0.002741	0.005051	0.990745	0.83965
				BSFC	0.003387	0.0073412			0.997845	0.99334
				CO	0.003457	0.0057421			0.99864	0.97458
				NOx	0.002471	0.0056710			0.99572	0.89457
				HC	0.000716	0.0016451			0.99121	0.9143
				Smoke	0.000104	0.0004510			0.99475	0.92548
Bayesian	sigmoid	800	32	BTE	0.005423	0.009471	0.004872	0.009877	0.9814	0.99077
				BSFC	0.004891	0.007510			0.99742	0.99875
				CO	0.003147	0.009875			0.99586	0.89451
				NOx	0.005124	0.014785			0.83965	0.99098
				HC	0.005241	0.008523			0.99334	0.98854
				Smoke	0.005412	0.009100			0.97458	0.99078
Bayesian	Relu	200	8	BTE	0.019250	0.003781	0.008391	0.009589	0.91470	0.89587
				BSFC	0.007812	0.029320			0.99412	0.90015
				CO	0.001563	0.00201			0.98451	0.87481
				NOx	0.010703	0.008356			0.91547	0.83965
				HC	0.005783	0.007489			0.90120	0.99334
				Smoke	0.005236	0.006583			0.94120	0.97458
Bayesian	Relu	400	16	BTE	0.009892	0.007457	0.005804	0.008655	0.978457	0.89457
				BSFC	0.006671	0.01739			0.97771	0.8841
				CO	0.001034	0.000504			0.94572	0.78452
				NOx	0.001054	0.006971			0.99098	0.8624
				HC	0.008752	0.012745			0.98854	0.84571
				Smoke	0.007425	0.006872			0.99078	0.97456
Bayesian	Relu	600	24	BTE	0.000192	0.026547	0.0135056	0.010712	0.89587	0.9012
				BSFC	0.012451	0.01542			0.90015	0.8923
				CO	0.003422	0.014257			0.87481	0.8845
				NOx	0.002062	0.001278			0.97844	0.8245
				HC	0.028722	0.005522			0.97771	0.9875
				Smoke	0.034210	0.001253			0.94572	0.9947
Bayesian	Relu	800	32	BTE	0.014620	0.021789	0.004450	0.006210	0.7895	0.99578
				BSFC	0.003245	0.003145			0.98678	0.9964
				CO	0.000990	0.006235			0.98247	0.9615
				NOx	0.000068	0.001642			0.97173	0.99784
				HC	0.003258	0.002241			0.99318	0.78956
				Smoke	0.004520	0.002212			0.98745	0.91457



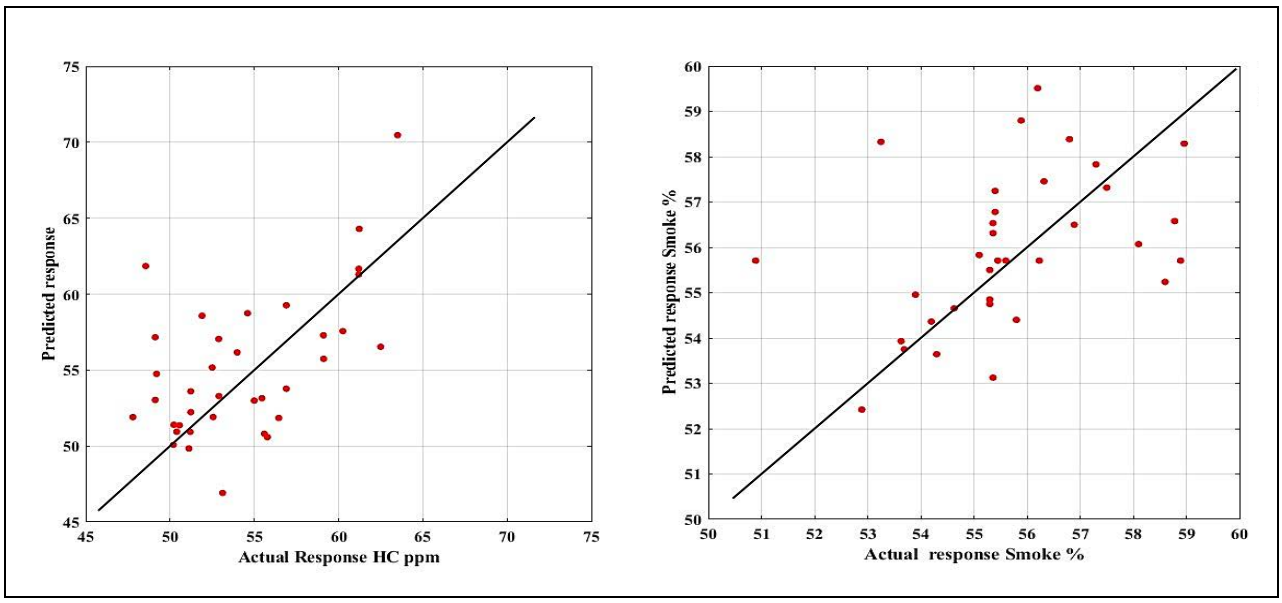


Fig. 10: ANN predictions for the output responses (experimental vs. forecasted)

The findings highlight that injection pressure alone cannot mitigate smoke emissions; optimal nozzle geometry, injector design, and timing are critical for reducing particulate matter (Damaik *et al*. 2018; Thamizhvel *et al.* 2020). Configurations like CR17.5IT22F1 are effective for meeting emission standards while ensuring efficient combustion. Although lemongrass biodiesel possesses higher unsaturation and oxygen content—factors that promote cleaner and more complete combustion—these same properties contribute to a slightly lower cetane number, resulting in a longer ignition delay. Its moderate viscosity facilitates improved atomization compared to more viscous conventional biodiesels; however, its lower energy content limits peak thermal efficiency. Overall, lemongrass biodiesel offers cleaner combustion characteristics but exhibits slightly reduced engine performance when compared to saturated biodiesel fuels. It was selected for this study due to its renewable origin, oxygenated molecular structure, and potential to reduce hydrocarbon emissions, smoke opacity, and dependence on fossil fuels. Additionally, its wide availability, biodegradability, and high suitability for esterification reinforce its promise as a sustainable alternative fuel.

4.6 Analysis of ANN

ANN network training was conducted using different optimizers and activation functions, with varying epochs and neuron counts, and the results are outlined in Table 4.

The Adam optimizer, combined with a sigmoid activation function in the hidden layer, outperforms other training optimizers and activation functions by achieving elevated correlation (r) and inferior validation MSE (Chizoo *et al*. 2019). The best network configuration is outlined in Table 5. This study determined that 32 neurons are needed to achieve the lowest MSE. The trend of the correlation (r) shows a strong relationship between all output variables and the input variables. The network predictions for test cases, along with the corresponding experimental results, are presented in Figure 10. The r and MSE values for CI engine parameters are 0.9924, 0.9944, 0.99488, 0.99124, and 0.9952, and 0.00016, 0.00042, 0.00021, 0.00018, and 0.00108 for NOX, HC, CO2, BTE, and BSFC, respectively.

Table 5. ANN model ideal configuration

Outcome neurons	6
Hidden neurons	32
Input neurons	4
Scaled range	0 to 1
Activation functions	Sigmoid, ReLu, Tanh
Optimizer	Bayesian
Epochs	r and MSE
No. of epochs	600
Data normalization	Scaler Min Max

The series of graphs (Fig. 10) compare the actual and forecasted values for diverse engine efficiency metrices, including BTE, BSFC, CO, NOx, HC, and Smoke opacity. Each graph features the actual outcome on the x-axis and the forecasted outcome on the y-axis, with a diagonal line representing perfect alignment.

- For thermal efficiency, the actual and forecasted values range from 25.5% to 30%, with most points clustered between 27.5% and 29%. Slight deviations occur, with underestimations or

overestimations of 0.5%–1%, but overall, the model demonstrates good predictive accuracy. In the BSFC graph, actual values span from 0.25 to 0.4 kg/kWh, while predicted values range from 0.28 to 0.46 kg/kWh. The model performs better at higher BSFC levels, but overpredictions are evident, especially in the upper range.

- For CO emissions, the actual values range from 0.35% to 0.6%, and predicted values range from 0.3% to 0.65%. While midrange predictions (0.45%–0.55%) align well with actual values, deviations are noticeable at the extremes, with underpredictions at lower CO levels and overpredictions at higher levels. Similarly, for NOx emissions, the actual and predicted values range from 210 ppm to 280 ppm. Most points cluster in the midrange (230–260 ppm), with increasing scatter at extreme values, reflecting reduced model reliability.

- The HC emissions graph shows actual and predicted values between 45 ppm and 75 ppm. The model performs well at lower levels (45–50 ppm), but accuracy decreases at higher values (70–75 ppm), with deviations reflecting both overpredictions and underpredictions. For Smoke opacity, both actual and predicted values range from 50% to 60%, with consistent predictions in the midrange (54%–58%). However, underpredictions dominate at lower values (50%–52%), while errors are more balanced at higher values.

- Overall, the models exhibit reasonable predictive accuracy, particularly in the midranges of the parameters. However, deviations at extreme values highlight areas for improvement, such as refining the models to better handle variability, adding features, or addressing biases in predictions.

5. CONCLUSIONS

- Diesel consistently outperforms biodiesel in key performance indicators. It achieves higher brake thermal efficiency (BTE), with values ranging from 28.55% to 29.5% at 260 bar, compared to biodiesel's 26.4% to 28.4%, due to its elevated heating feature and enhanced atomization. Diesel (F0) also exhibits lower BSFC, ranging from 0.29–0.32 kg/kWh at 240 bar, while biodiesel's BSFC is 14–35% higher, at 0.42 kg/kWh, due to its lower energy density.

- Lemongrass biodiesel exhibited a slightly longer ignition delay than diesel due to its lower cetane number and higher unsaturation. However, its oxygen content aided combustion, making it a viable alternative despite the marginal delay.

- In terms of emissions, diesel produces less carbon monoxide (CO), with values ranging from 0.4166% to 0.4236% at 260 bar, while biodiesel emits 0.45% to 0.51%, benefiting from oxygen content but hindered by its higher viscosity.

- However, lemon grass biodiesel generates higher nitrogen oxide (NOx) emissions, ranging from 244.21 to 249.00 PPM at 260 bar, compared to diesel’s

- 237.71–249.23 PPM, primarily due to its oxygen-rich composition.

- Biodiesel also achieves lower hydrocarbon (HC) emissions, with a minimum of 47.8 PPM at 260 bar, thanks to improved combustion, while diesel emissions are higher. Lastly, biodiesel shows improved smoke opacity, with the lowest opacity of 53.9% at 260 bar, owing to improved fuel-air mixing and optimized injection timing.

- ANN model demonstrates reasonable predictive accuracy for engine performance parameters, with strong alignment between actual and predicted values in midranges. For SFC, BTE, NOx, smoke opacity, HC, and CO, deviations are generally within 0.5%–1% or equivalent ranges, but accuracy decreases at extreme values, highlighting the need for refinements to handle variability and reduce prediction biases.

FUNDING

This research received no specific grant from any funding agency in the public, commercial, or not-for-profit sectors.

CONFLICTS OF INTEREST

The authors declare that there is no conflict of interest.

COPYRIGHT

This article is an open-access article distributed under the terms and conditions of the Creative Commons Attribution (CC BY) license (http://creativecommons.org/licenses/by/4.0/).

REFERENCE

Arunprasad, S. and Balusamy, T., Experimental investigation on the performance and emission characteristics of a diesel engine by varying the injection pressure and injection timing using mixed biodiesel, *Int. J. Green Energy*, 15, 376–384 (2018). https://doi.org/10.1080/15435075.2018.1464923

Babu, D., Thangarasu, V. and Ramanathan, A., Artificial Neural Network Approach on Forecasting Diesel Engine Characteristics Fuelled with Waste Frying Oil Biodiesel, *Appl. Energy*, 263, 114612(2020). https://doi.org/10.1016/j.apenergy.2020.114612

Bahri, B., Shahbakhti, M. and Aziz, A. A., Real-Time Modeling of Ringing in HCCI Engines Using Artificial Neural Networks, *Energy*, 125, 509–518(2017). https://doi.org/10.1016/j.energy.2017.02.137

Channapattana, S., Pawar, A. and Kamble, P. G., Optimisation of Operating Parameters of DI-CI Engine Fueled with Second Generation Bio-Fuel and Development of ANN Based Prediction Model, *Appl. Energy*, 187, 84–95(2017). https://doi.org/10.1016/j.apenergy.2016.11.030

Chizoo, E., OkechukwuDonminic, O., Akuzuouwaoma, O. and EkechiOgah, O., Multi-Input Multi-Output (MIMO) ANN and Nelder-Mead's Simplex Based Modeling of Engine Performance and Combustion Emission Characteristics of Biodiesel-Diesel Blend in CI Diesel Engine, *Appl. Therm. Eng*., 151, 100-114(2019). https://doi.org/10.1016/j.applthermaleng.2019.01.101

Damaik, N., Ong, H. C., Tong, C. W., Mahlia, T. M. I. and Silitonga, A. S., A review on the engine performance and exhaust emission characteristics of diesel engine fueled with biodiesel blends, *Environ. Sci. pollut. Res. Int*., 25(16), 15307-25(2018). https://doi.org/10.1007/s11356-018-2098-8

Datta, A. and Mandal, B. K., A Comprehensive Review of Biodiesel as an Alternative Fuel for Compression Ignition Engine, *Renew. Sustain. Energy Rev.*, 57, 799–821(2016). https://doi.org/10.1016/j.rser.2015.12.170

Dhar, A. and Agarwal, A., Performance, emissions and combustion characteristics of karnaja biodiesel in a transportation engine, *Fuel*, 119, 70–80(2014). https://doi.org/10.1016/j.fuel.2013.11.002

Dwivedi, G. and Sharma, M. P., Prospects of Biodiesel from Pongamia in India, *Renew. Sustain. Energy Rev*., 32, 114–122(2014). https://doi.org/10.1016/j.rser.2014.01.009

Esonye, C., Onukwuli, O. D., Ofoefule, A. U. and Ogah, E.O., Multi-Input Multi-Output (MIMO) ANN and Nelder-Mead's Simplex Based Modeling of Engine Performance and Combustion Emission Characteristics of Biodiesel-Diesel Blend in CI Diesel Engine, *Appl. Therm. Eng*., 151, 100–114(2019). https://doi.org/10.1016/j.applthermaleng.2019.01.101

Ilangkumaran, M., Sakthivel, G. and Nagarajan, G., Artificial Neural Network Approach to Predict the Engine Performance of Fish Oil Biodiesel with Diethyl Ether Using Back Propagation Algorithm, *Int. J. Ambient Energy*, 37, 446–455(2016). https://doi.org/10.1080/01430750.2014.984082

Krishnamoorthi, M. and Malayalamurthi, R., Engine Characteristics Analysis of Chaulmoogra Oil Blends and Corrosion Analysis of Injector Nozzle Using Scanning Electron Microscopy/Energy Dispersive Spectroscopy, *Energy*, 165, 1292–1319(2018). https://doi.org/10.1016/j.energy.2018.10.112

Maurya, R. K., Saxena, M. R., Rai, P. and Bhardwaj, A., Effect of compression ratio, nozzle opening pressure, engine load, and butanol addition on nanoparticle emissions from a non-road Diesel engine, *Environ. Sci. Pollut. Res.*, 25(15), 14674–14689(2018). https://doi.org/10.1007/s11356-018-1644-8

Nirmala, N., Dawn, S. S. and Harindra, C., Analysis of Performance and Emission Characteristics of Waste Cooking Oil and ChlorellaVariabilis MK039712.1 Biodiesel Blends in a Single Cylinder, Four Strokes Diesel Engine, *Renew. Energy*, 147, 284–292(2020). https://doi.org/10.1016/j.renene.2019.08.133

Odufuwa, O. Y., Tartibu, L. K. and Kusakana, K., Effects of soybean biodiesel on a DI diesel engine performance, emissions and combustion Characteristics, *Fuel*, 115, 875-83(2014). https://doi.org/10.1016/j.fuel.2012.10.081

Qi, D. H., Chen, H., Geng, L. M. and Bian Z. H. Y., Experimental studies on the combustion characteristics and performance of a direct injection engine fueled with biodiesel/ diesel blends, *Energy convers. Manage*., 51, 2985–92(2010). https://doi.org/10.1016/j.enconman.2010.06.042

Ramalingam, K., Kandasamy, A., Balasubramanian, D. and Palani, M., Forcasting of an ANN model for predicting behaviour of diesel engine energised by a combination of two low viscous biofuels, *Environ. Sci. Pollut. Res*., 27, 24702–24722(2020). https://doi.org/10.1007/s11356-019-06222-7

Shafay, A. S., Alqsair, U. F., Abdel, S. M. and Gad, M. S., Artificial neural network prediction of performance and emissions of a diesel engine fueled with Palm Biodiesel, *Sci. Rep.*, 12(1), 9286(2022). https://doi.org/10.1038/s41598-022-13413-9

Silitong, A. S., Masjuki, H. H., Hwai, C. O., Dharma, S., Kusumo, F., Siswantoro, J., Milano, J., Daud, K., Mahlia, K. and Bambang. S., Evaluation of the engine performance and exhaust emissions of biodiesel – bioethanol –diesel blends using kernel-based extreme learning machine, Energy,159, 1075 – 87(2018). https://doi.org/10.1016/j.energy.2018.06.202

Soukht, S. H., Taghavifar, H. and Jafarmadar, S., Experimental and Numerical Consideration of the Effect of CeO2 Nanoparticles on Diesel Engine Performance and Exhaust Emission with the Aid of Artificial Neural Network, *Appl. Therm. Eng*., 113, 663–672(2017). https://doi.org/10.1016/j.applthermaleng.2016.11.044

Teoh, Y. H., How, H. G., Sher, F. and Le, T. D., Optimization of fuel injection parameters of moringaoleifera biodiesel-diesel blend for engine-out-responses improvements, *Symmetry,* 13(6), 982(2021). https://doi.org/10.3390/sym13060982

Thamizhvel, R., Performance on biomass gasification of groundnut shell in down draft fixed bed reactor, *Int. J. Food Eng*., 10(3), 4963–4970(2020). https://doi.org/10.24247/IJMPERDJUN2020470

Vinod, R. S. and Dheikshith, R., Performance and emission characteristics of diesel engine fuelled with cashew nut Shell Oil & optimizing the operating parameters using response surface methodology. IOP Conference Series, *Earth Environ. Sci.,* 1161(1), 012002(2023). https://doi.org/10.1088/1755-1315/1161/1/012002

Vinodraj, S. R., Arularasan, D. and Karthikeyan, Impact of non-edible biodiesel (Juliflora oil seed) on CI engine – Combustion, performance and emission features, *Mater. Today Proce*., 2214-7853(2023). https://doi.org/10.1016/j.matpr.2023.05.306

Yahya, S., Muhamad Wahab, S. K. and Harun, F. W., Optimization of biodiesel production from waste cooking oil using Fe-Montmorillonite K10 by response surface methodology, *Renewable Energy* 157, 164-172(2020). https://doi.org/10.1016/j.renene.2020.04.149